

# Real-time material quality prediction, fault detection, and contamination control in AlGaIn/GaN high electron mobility transistor metalorganic chemical vapor deposition process using *in situ* chemical sensing

Soon Cho<sup>a)</sup> and Gary W. Rubloff<sup>b)</sup>

Department of Materials Science and Engineering and Institute for Systems Research, University of Maryland, College Park, Maryland 20742

Michael E. Aumer, Darren B. Thomson, and Deborah P. Partlow

Advanced Materials and Semiconductor Device Technology Center, Northrop Grumman Electronic Systems, Linthicum, Maryland 21090

(Received 7 January 2005; accepted 20 June 2005; published 15 August 2005)

Gallium nitride and its alloys promise to be key materials for future heterojunction semiconductor devices aimed at high frequency, high power electronic applications. However, manufacturing for such high performance products is challenged by reproducibility and material quality constraints that are notably higher than those required for optoelectronic applications. To meet this challenge, *in situ* mass spectrometry was implemented in AlGaIn/GaN/AlN metalorganic chemical vapor deposition processes as a real-time process and wafer state metrology tool. In particular, the various pregrowth gas phase impurity levels within the reactor, measured by mass spectrometry in real time, were correlated to photoluminescence band-edge and deep-level properties measured postprocess. Band-edge intensities increased and deep-level intensities decreased with lower oxygen-containing impurity levels in the pregrowth environment. These real-time indications of oxygen impurity incorporation were used for fault detection and to optimize preprocess reactor conditioning involving degassing of the wafer susceptor and furnace liner elements. Because this *in situ* sensing provides a control on contaminants to assure high material quality and a fault detection capability as well, it is now implemented routinely for both purposes. These real-time contamination control and fault detection strategies complement an overall advanced process control program for GaN-based semiconductor manufacturing, offering a systematic methodology to improve the product quality of GaN-based electronic devices. © 2005 American Vacuum Society. [DOI: 10.1116/1.2006110]

## I. INTRODUCTION

In recent years, GaN and AlGaIn-based materials have been recognized as key materials for future semiconductor devices aimed at high frequency and high power electronic operation (e.g., radar applications).<sup>1–3</sup> Unlike the rapidly expanding applications for GaN technology in optoelectronics (e.g., light emitting diodes), such high performance electronic applications place greater demands on the material quality which is needed for desired device performance. However, despite the potential of these materials, currently the level of control and reproducibility in these processes is inadequate for high volume manufacturing. This is attributed to the complexity of the process chemistries involved, the earlier stage of the technology's evolution, and the consequent absence of emphasis on advanced process control (APC).

On the other hand, APC has already been widely accepted in the Si ultralarge scale integrated (ULSI) industry, both in terms of fault detection and classification (FDC), and course

correction.<sup>4,5</sup> Our research group has been an active contributor in various aspects of APC, especially in the use of real-time *in situ* chemical sensors for both FDC and course correction.<sup>6–16</sup> In view of the relevant challenges currently facing the development of GaN-based processes for manufacturing in electronic applications, we have applied similar APC approaches based on our past experience in Si-based processes in hopes of achieving process reproducibility sufficient for manufacturing.<sup>17,18</sup> We have employed *in situ* mass spectrometry in AlGaIn/GaN/AlN metalorganic chemical vapor deposition (MOCVD) processes to grow high electron mobility transistor (HEMT) heterostructures on semi-insulating SiC for high frequency/power electronic devices. In this article we report the application of real-time, *in situ* sensing to material quality prediction, fault detection, and contaminant control, as extensions of our prior metrology and crystal growth results in GaN-based systems.<sup>19,20</sup>

Real-time course correction for the critical AlGaIn cap layer thickness (~1% control of ~20 nm) has been enabled by metrologies based on integration of methane and ethane byproduct signals measured by mass spectrometer.<sup>19</sup> In addition, both FDC and course correction of GaN epilayer crystal quality (as verified by postprocess x-ray diffraction to 1%–5% precision) have been made possible by the methane/

<sup>a)</sup>Current affiliation: Intel Corporation; electronic mail: soon.cho@intel.com

<sup>b)</sup>Author to whom correspondence should be addressed; electronic mail: rubloff@isr.umd.edu

ethane byproducts ratio monitored in real time during growth.<sup>20</sup> Both the AlGaIn cap layer thickness control and GaN epilayer crystal quality control are needed during the respective film growth periods of the process. These real-time control approaches provide a number of important advantages compared to the run-to-run control technology which is already a mature component of APC in the industry—e.g., real-time control can compensate for random short-term variability that occurs within a process in addition to the long-term systematic process drift. We can go beyond real-time control by implementing measures of fault detection and contamination control described here that prepare an optimal growth environment prior to initiation of the actual growth. This increases the chances of producing better quality material in a systematic manner, for example with reduced gas phase impurity levels within the reactor. These various components of APC (i.e., course correction, FDC, and contamination control) work to complement one another as demonstrated in this article and our previous publications.<sup>19,20</sup>

## II. EXPERIMENTS

### A. HEMT heterostructure growth by MOCVD

Details of the experimental process conditions and equipment descriptions are published elsewhere<sup>20</sup> and only a summary is presented here. All experiments were carried out within a water-cooled quartz-wall reactor (custom designed), which includes a quartz liner inside a double quartz furnace wall. The system was equipped with a commercial gas delivery system supplied by EMF Ltd. Reactants [NH<sub>3</sub>, trimethylaluminum (TMA), and trimethylgallium (TMG)] with the carrier gas (H<sub>2</sub>) were delivered through two quartz delivery tubes fused to a custom designed quartz showerhead. In particular, the metalorganic precursors (TMA and TMG) and NH<sub>3</sub> were kept separated in their respective delivery tubes until they reached the showerhead, at which point they intermixed uniformly within the showerhead before being delivered to the wafer region below. Single wafer substrate (2 in. diam semi-insulating SiC from Cree) was placed on the SiC-coated graphite susceptor. The susceptor was inductively heated at 10 kHz to provide heating for the film growth to occur on the wafer. The residual process gases were continuously pumped away through the exhaust lines located at both ends of the reactor, connected to a common rotary vane pump.

All three layers of the HEMT heterostructure (AlGaIn/GaN/AlN layers on 2 in. semi-insulating SiC substrate) were grown sequentially within the same process, and an *in situ* mass spectrometer was used to monitor the progress in real time. In fact, the data discussed in this article are from the same HEMT heterostructure growth runs presented in our previous publication on real-time product crystal quality prediction.<sup>20</sup> Details of the exact equipment configurations and process conditions used are described in the same article and are not repeated here.

### B. Real-time *in situ* process sensing by mass spectrometry

The schematic layout of the mass spectrometer sampling system, integrated to the MOCVD tool, is published elsewhere.<sup>20</sup> The process and residual gases were sampled directly from the reactor downstream via a 1/16 in. o.d.  $\times$  0.010 in. i.d.  $\times$  20 cm long stainless steel capillary, which resulted in a pressure drop from the process pressure of 50 Torr down to  $\sim$ 1 Torr behind the capillary. Most of this gas was then pumped away by a bypass differential pumping to the foreline of the diaphragm pump (backing pump for the mass spectrometer's turbomolecular pump), leaving only a small fraction of the gas to enter a 20  $\mu$ m i.d. orifice into the closed ion source region of the mass spectrometer (Inficon model CPM<sup>TM</sup>, 200 amu quadrupole mass spectrometer).

By using an appropriately sized capillary-orifice combination for the gas conductance network, the sampled gas pressure was reduced from the viscous flow regime (50 Torr) to the molecular flow regime ( $\sim$ 1 Torr). The bypass differential pumping technique enabled us to actively withdraw gases from the process through the sampling system. Both of these sampling techniques, as well as the location of the sampling capillary (i.e., within the main gas flow downstream to the growth reaction), were critical in achieving adequate response time in process sensing.

The W filament current in the closed ion source was kept at 200  $\mu$ A, while the electron energy was maintained at 40 eV. This provided adequate sensitivity and minimum parasitic reactions within the closed ion source region. Electron multiplier detection was used at an acceleration voltage of 835 V to enhance and maintain the signal-to-noise ratio run to run.

### C. Postprocess material characterization

The samples grown on SiC substrates as described in the preceding sections were examined using a number of post-process characterization techniques, including photoluminescence (PL), x-ray diffraction (XRD), and x-ray reflectance. In particular, the PL characterization (by Accent RPM2000<sup>TM</sup> system) provided multiple important semiconductor material quality metrics in a relatively timely manner. A 266 nm pulsed laser was incident on the sample and an ultraviolet-enhanced charge coupled device camera captured the spectrum. The *r*- $\theta$  stage allowed the entire wafer mapping in minutes at 30 pts/s and a resolution of 1 mm. The spectral scan mode provided information on the characteristic peaks at both the band-edge (364.6 nm) and deep-level (550.1 nm) for the GaN layer, where the band-edge intensity reflects the ratio of radiative to nonradiative recombination, and the deep-level (or yellow luminescence) is related to defects, impurities, and mid-gap/surface states within the material. Additional information such as the full-width at half-maximum peak height for crystal quality and the alloy composition for the AlGaIn cap layer were obtained from the same measurement. The white light spectrum mode provided the GaN epilayer thickness from the interference fringe separation. Here, we used the band-edge and deep-level intensities aver-

aged over the 2 in. wafer as measures of average material quality, and the similarly averaged epilayer thickness to deduce the average growth rate.

### III. RESULTS

#### A. Real-time *in situ* metrology development

Details of the mass spectrometry sensing and metrology development are published elsewhere<sup>19,20</sup> and only a summary is presented here. *In situ* mass spectrometry sensing of the 50 Torr MOCVD growth process as described above provided dynamic, real-time gas phase chemical signals as a function of the process cycle. Characteristic ion current signals were obtained for H<sub>2</sub> (carrier gas), NH<sub>3</sub> (column V precursor), N<sub>2</sub> (fragmentation product from NH<sub>3</sub>), H<sub>2</sub>O (background impurity), CH<sub>4</sub> (reaction byproduct), C<sub>2</sub>H<sub>6</sub> (reaction byproduct), C (background impurity), O<sub>2</sub> (background impurity), and other yet unknown impurity species (e.g., at 55 amu). In particular, it is demonstrated in this article that the background impurity levels measured at amu's 18 (H<sub>2</sub>O), 32 (O<sub>2</sub>), and 55 (unknown impurity) correlate to the PL band-edge and deep-level intensities with reasonable precision (~5%).

#### B. Real-time prediction of GaN photoluminescence qualities and metrology

In our previous publications, it was demonstrated that the real-time methane/ethane ratio enabled prediction of GaN epilayer crystal quality during growth to a precision 2%–5%, which was verified by the postprocess measurement of crystal quality by XRD.<sup>20</sup> Here we demonstrate that the same methane/ethane ratio metric, obtained during GaN epitaxy, can also predict PL band-edge intensity to within ~5% precision. This is shown in Fig. 1 for the same set of four runs, for which the crystal quality correlation was demonstrated. Moreover, the correlation is such that by going to lower methane/ethane ratio we improve material quality as seen in both XRD and PL. This has further implications in terms of the intrinsic chemistry, and is discussed in Sec. IV.

*In situ* mass spectrometry sensing also allowed monitoring of the background impurity species during GaN epitaxy as discussed already in the previous section. In particular, we focused our attention on the gas phase residual H<sub>2</sub>O and O<sub>2</sub> because they are common impurities in other semiconductor processes, and in part because oxygen (from either H<sub>2</sub>O or O<sub>2</sub>) is known to act as an unintentional shallow donor in GaN along with other types of defects such as nitrogen vacancies.<sup>21</sup> Correlations showed that the PL band-edge intensity suffered (i.e., lower) with more residual H<sub>2</sub>O present during GaN epitaxy and the PL deep-level intensity suffered (i.e., higher) with more residual O<sub>2</sub> present during GaN epitaxy.<sup>17,18</sup> Therefore, we learned that achieving a low gas phase impurity condition within the reactor is critical for high quality GaN material growth. We also realized that such conditions must be established prior to the GaN growth step itself because there is little room for course correction as far as removing the impurities in a timely fashion is concerned.

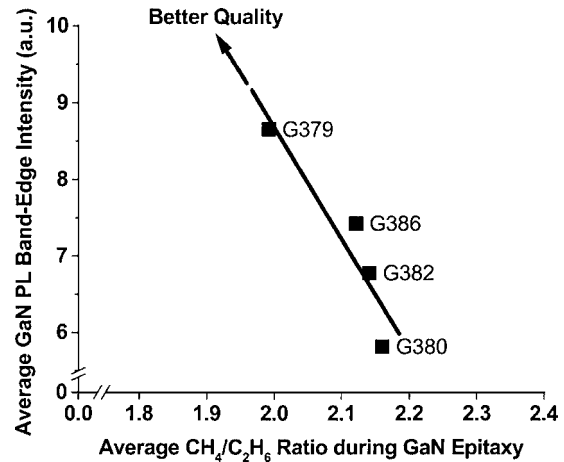


FIG. 1. Real-time prediction of GaN PL band-edge intensity during growth based on *in situ* mass spectrometry measurement of methane/ethane byproducts ratio (precision 4.8%). The four runs shown here correspond to the same four runs presented in our previous publication on crystal quality prediction, (see Ref. 20) where it was shown that the same methane/ethane ratio metric predicts GaN epilayer crystal quality to 3.5% verified by post-process XRD. Moreover, the correlation is such that by going to lower methane/ethane ratio we improve material quality as seen in both XRD and PL.

Hence, our attention was directed to the pregrowth steps, where we still have a chance to effectively reduce the impurity levels within the reactor prior to the actual film growth. In particular, we focused on the pregrowth reactor purge steps (room temperature purge, heating, followed by high temperature purge), where we attempt to bake away the impurities with high temperature (~1100 °C) and purging gas (H<sub>2</sub>). Details of these pregrowth steps are described elsewhere.<sup>20</sup> Progress of the reactor purge is monitored in real time using the mass spectrometry, and the impurity levels were noted at the end of the high temperature purge step, which occurred immediately prior to the actual HEMT heterostructure growth, for correlation to postprocess PL quality measurements. Not surprisingly, the residual H<sub>2</sub>O level measured at that point was found to correlate to the PL band-edge intensity measured postprocess as shown in Fig. 2. Better quality material (as seen in higher band-edge intensity) was obtained when the pregrowth residual H<sub>2</sub>O level was lower, with the correlation accurate to ~7%. Note that these results include the same set of runs as shown in Fig. 1.

PL band-edge intensity was also found to correlate to another impurity measured at 55 amu (unknown specie) as shown in Fig. 3. However, in this case, better quality material (as seen in higher band-edge intensity) was obtained with higher (not lower) impurity level detected prior to growth. Further study is required to determine the exact identity of the unknown specie at 55 amu. It is conjectured that this specie is some type of residual impurity compound formed by a combination of C, H, and O, because its steadily decreasing behavior through the entire process cycle parallels that for C and O.

High band-edge intensity alone does not mean anything unless accompanied by low deep-level (yellow) lumines-

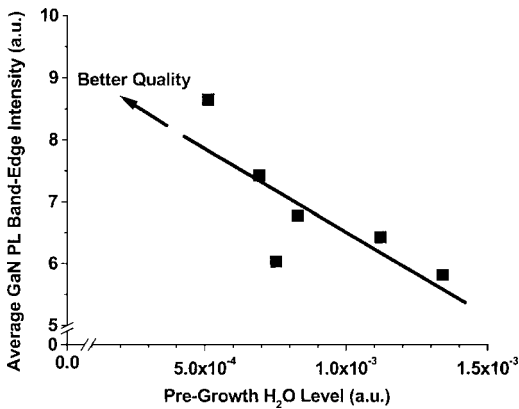
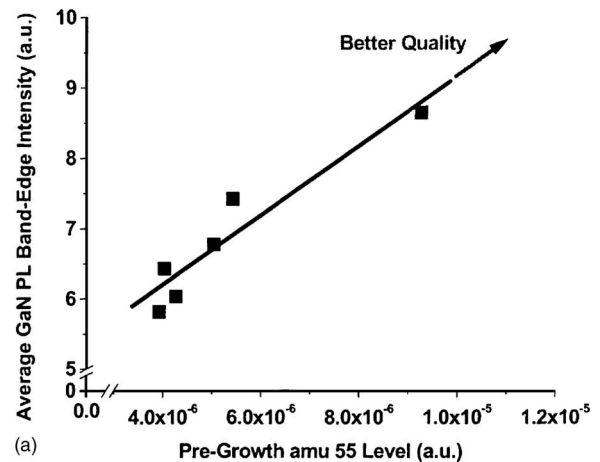


FIG. 2. Correlation of the gas phase residual  $\text{H}_2\text{O}$  level within the pregrowth reactor to the GaN PL band-edge intensity measured postprocess. Better quality material (as seen in higher band-edge intensity) was obtained when the pregrowth residual  $\text{H}_2\text{O}$  level was lower with the correlation accurate to 6.6% here.

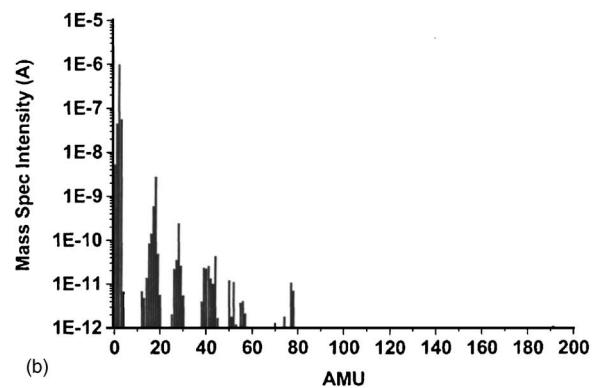
cence. Therefore, the two must be optimized concurrently: typically resulting in a band-edge to deep-level ratio of  $>1000$ . We found that by normalizing the pregrowth residual  $\text{O}_2$  level to the epilayer growth rate (both of which can be obtained in real time from mass spectrometer), PL deep-level can be predicted as shown in Fig. 4. Better quality material (as seen in lower deep-level intensity) was obtained when the pregrowth residual  $\text{O}_2$  level was lower and the growth rate was lower, with the correlation accurate to  $\sim 19\%$ . Although the correlation here is less precise compared to the case of PL band-edge intensity, this offers an important means to predict and possibly control GaN deep-level concurrent with the band-edge intensity, because the two parameters put together are critical as a measure of GaN material quality.

### C. Additional real-time fault detection

The same mass spectrometer sensor that provides us with all of these useful metrology models for process control<sup>19,20</sup> and pregrowth contamination control (as described in this article) can also be used to drive fault detection. In fact, mass spectrometer has been by far the most pervasive chemical sensor for successful fault detection in APC in the Si ULSI industry. Here, we developed a number of such fault detection applications based on clear chemical signatures for process and equipment faults which potentially lead to unacceptable product quality. For instance, we monitored the progress of the reactor purge during the pregrowth steps as described in the previous section and shown in Fig. 5. Part (a) of the figure shows  $\text{H}_2\text{O}$  vapor desorbing from the unconditioned walls of a brand new liner as soon as the temperature ramp begins. In addition, we observed impurity desorption from a dirty susceptor in the form of  $\text{N}_2$  during the high temperature purge, also shown in part (a). However, such impurity evolutions were not observed with a well conditioned liner and a clean susceptor as shown in part (b). These kinds of real-time indications as in part (a) clearly correlated to unacceptable material quality by PL, and they indicated a need for measures to correct the root cause.



(a)



(b)

FIG. 3. (a) Correlation of the gas phase residual impurity level, measured at 55 amu, within the pregrowth reactor to the GaN PL band-edge intensity measured postprocess. Better quality material (as seen in higher band-edge intensity) was obtained with higher (not lower) impurity level detected prior to growth with the correlation accurate to 10% here. (b) Further study is required to determine the exact identity of the unknown specie at 55 amu and its effect on the process. However, the objective of the current publication was to identify working metrics for immediate implementation of process fault detection and material quality prediction. A sample full spectra taken from the pregrowth reactor is shown as a reference. Mass resolution capability was limited to 1 amu, and for optimum response time required for real-time process control only a selected set of amus were monitored at 2, 13, 17, 18, 26, 27, 28, 32, and 55 amu.

While adequate conditioning of a brand new liner could be achieved simply by extending the duration of the pregrowth purge steps, faults based on cracking of, or impurity coatings on, the susceptor required more extensive solutions to correct them since those kinds of impurities (C from the exposed graphite or other undesirable impurities desorbing from the susceptor) tend to be from a semi-infinite source which degrades film quality. Thus, we implemented replacement of the susceptor followed by a dedicated bakeout conditioning run prior to the next actual HEMT heterostructure growth run. The solution measures described here resulted in a well conditioned liner and a clean susceptor, from which no signatures of faults were observable as shown in Fig. 5(b), and they usually resulted in improvement in product material quality in the subsequent runs.

There have also been cases where the upstream mass flow controllers (MFCs) for delivering various gases into the re-

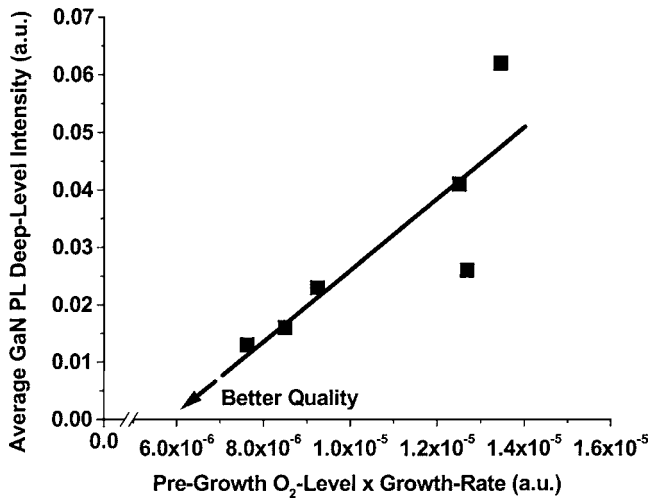


FIG. 4. Correlation of the gas phase residual  $O_2$  level within the pregrowth reactor to the GaN PL deep-level intensity measured postprocess. Better quality material (as seen in lower deep-level intensity) was obtained when the pregrowth residual  $O_2$  level was lower with the correlation accurate to 19% here. Although the correlation here is less precise compared to the case of PL band-edge intensity, this offers an important means to predict and possibly control GaN deep-level concurrent with the band-edge intensity, because the two parameters put together are critical as a measure of GaN material quality.

actor failed in the middle of the growth process as shown in Fig. 6. In this case, failure of the  $NH_3$  MFC during GaN epilayer growth was detected by the mass spectrometry, while the main tool controller indicated a normal status. The real-time signatures indicating large disturbances (up to  $\sim 3$  orders of magnitude) in the  $NH_3$  concentration within the reactor were immediately noticed by the process engineer, and were followed by a series of manual tests as indicated by sections A, B, and C for trouble-shooting. Section A indicates a test where the isolation valve between the mass spectrometer and the reactor was closed for a period of  $\sim 2$  min. Stable  $NH_3$  signal (still remaining high due to the trapped volume within the sampling inlet of the sensor) during this period as well as the time scale for each sensing scan (10.353 s) confirmed that the disturbances were real physical effects and not electrical noise. Sections B and C indicate a series of MFC flow variation tests where the set point for the MFC flow rate was altered between a high value (80% for B) and a low value (40% for C). Results of the test indicate that the MFC failed to perform properly for low flow set point conditions. Needless to say, postprocess characterization results of the product material from this run were far from acceptable. The MFC in question was replaced immediately and both the sensor signals as well as the future product materials themselves indicated that the fault was successfully resolved.

Finally, Fig. 7 shows sensing during a run where the reaction byproduct ( $CH_4$  and  $C_2H_6$ ) levels were significantly lower than the usual. Again, this was immediately noticed by the process engineer monitoring the sensor output in real time. Although the unusually low byproduct levels do not necessarily correspond directly to precursor source depletion,

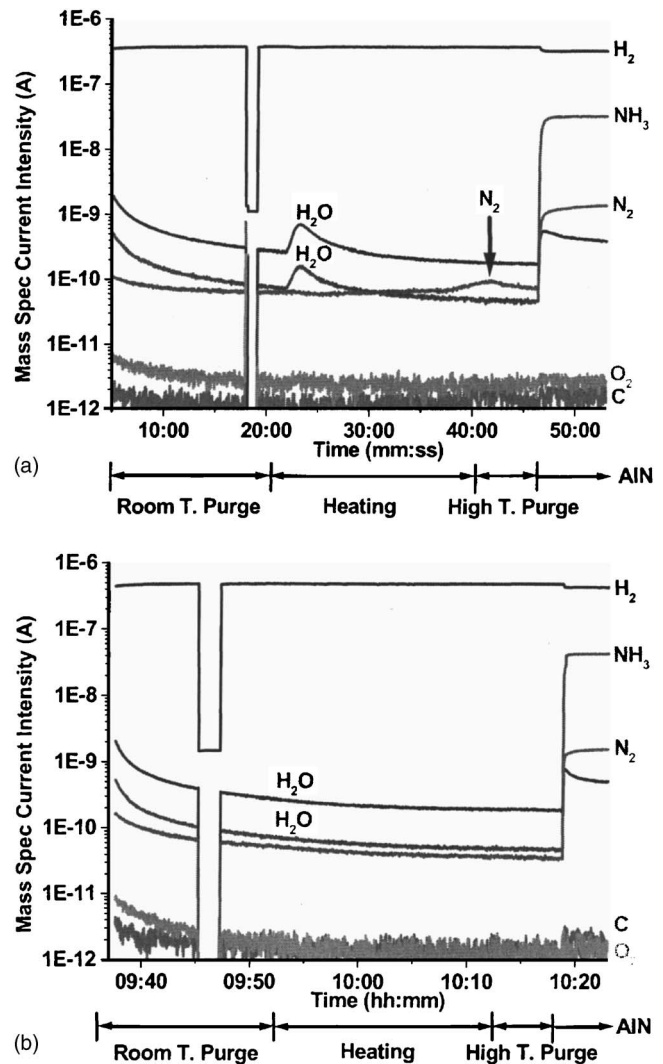


FIG. 5. Example of real-time fault detection based on clear chemical signatures for process and equipment faults which potentially lead to unacceptable product quality. (a) Desorption of  $H_2O$  vapor from the unconditioned walls of a brand new liner as soon as the temperature ramp begins, followed by desorption of impurity coating from a dirty susceptor in the form of  $N_2$  during the high temperature purge. (b) Such impurity evolutions were not observed with a well conditioned liner and a clean susceptor. These kinds of real-time indications as in (a) clearly correlated to unacceptable material quality by PL, and they indicated a need for measures to correct the root cause, such as through extended pregrowth contamination control and replacement of corresponding tool parts (e.g., susceptor). The cause of signal loss at  $\sim 18:00$  h in (a) and  $\sim 09:45$  h in (b) is an intentional feature (used for electron multiplier gain study) and may be ignored for the purposes of analyses here.

it certainly provides a useful real-time signature that leads to more in-depth fault classification in a timely manner. In this case, insufficient growth of product film seen postprocess matched the real-time fault detection by the sensor, and led to examination of a limited number of possible sources for the fault, which included precursor source depletion and excessive deposition within the showerhead. Once the root cause for the fault was identified—in this case precursor source depletion—an appropriate solution was implemented to correct the problem (i.e., immediate replacement of the precursor source bottle).

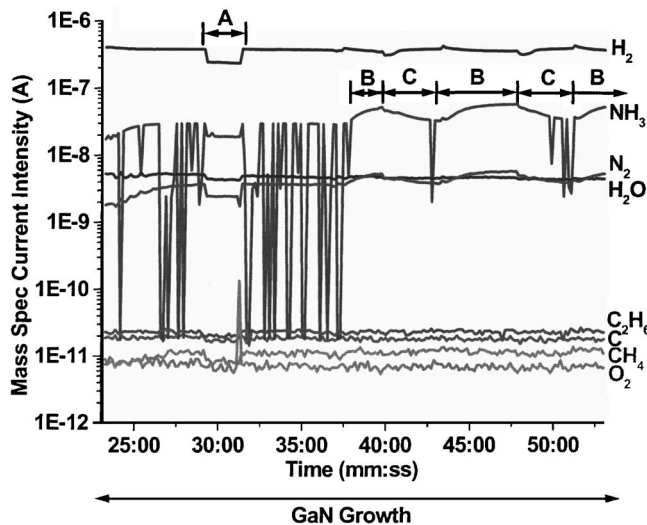


Fig. 6. Example of real-time detection of an equipment excursion in the middle of process that led to unacceptable material quality. Failure of an  $\text{NH}_3$  MFC was immediately detected by the mass spectrometry during GaN epilayer growth from the real-time signatures indicating large disturbances in the  $\text{NH}_3$  concentration within the reactor. Segment A indicates a manual test where the isolation valve between the mass spectrometer and the reactor was closed for a period of  $\sim 2$  min. Stable  $\text{NH}_3$  signal (still remaining high due to the trapped volume within the sampling inlet of the sensor) during this period as well as the time scale for each sensing scan (10.353 s) confirmed that the disturbances were real physical effects and not an electrical noise. Segments B and C indicate a series of MFC flow variation tests where the set point for the MFC flow rate was altered between a high value (80% for B) and a low value (40% for C). Results of the test indicate that the MFC failed to perform properly for low flow rate set point conditions. The MFC in question was replaced immediately and both the sensor signals as well as the future product materials themselves indicated that the fault was successfully resolved.

Normally, if the reactants are originally in the form of gas phase, the gas bottle pressures provide a means to closely follow their usage levels over time. However, in this case and in increasing number of semiconductor processes today, that is not the case. The metalorganic precursors (TMG and TMA), originally in the liquid phase and kept in temperature controlled bubblers, are delivered to the reactor via the saturated carrier gas ( $\text{H}_2$ ). Accurate monitoring of the run-to-run usage level becomes more difficult. We may be able to deduce it by monitoring the reactant and/or the reaction byproduct levels upstream or downstream of the wafer. One of the options may be the use of acoustic sensors, installed between the bubbler and the reactor, to monitor the precursor concentration in the upstream delivery line. This would also allow real-time closed-loop control to maintain desired level of concentration in the face of run-to-run drift in concentration due to changes in the liquid source vapor pressure with overtime usage.<sup>22</sup> Here, the mass spectrometer sensor monitoring the growth reaction far downstream of the wafer provided an additional capability to detect such faults in real time. Thus, although the former option may be a more elegant solution, the latter option is extremely attractive because it allows for multiple applications with both process- and wafer-state control, and other types of real-time fault detection applications at the same time with a single sensor.

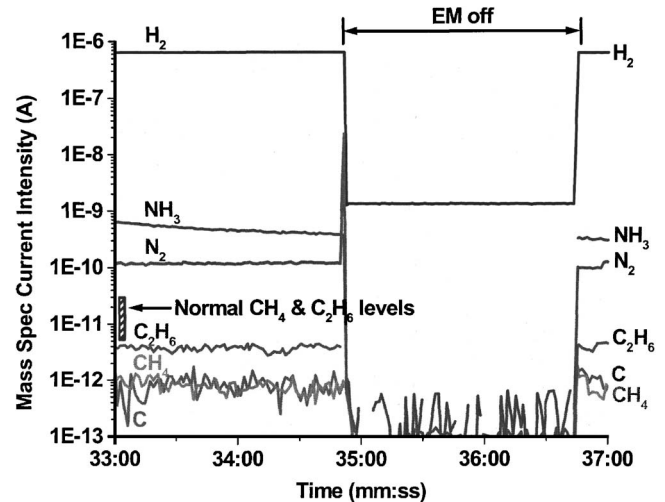


Fig. 7. Mass spectrometry sensing during a run where the reaction byproduct ( $\text{CH}_4$  and  $\text{C}_2\text{H}_6$ ) levels were significantly lower than the usual. This was correlated to the little growth of product film seen postprocess, which led to examination of a limited number of possible sources for the fault. Once the root cause was identified to be untimely precursor source depletion, the precursor source bottle was immediately replaced. The segment labeled “EM off” indicates a test where the mass spectrometer electron multiplier was turned off for  $\sim 2$  min and then turned back on to confirm that it was functioning properly.

Nevertheless, these kinds of *in situ* sensors have proven to be extremely valuable to drive fault detection as demonstrated here.

#### IV. DISCUSSION

One of the key results demonstrated here (Fig. 1) was that the same methane/ethane ratio metric from mass spectrometry used to predict GaN epilayer crystal quality (measured by XRD)<sup>20</sup> could also be used to predict PL band-edge intensity with similar quantitative precision ( $\sim 5\%$ ). Moreover, the correlation is such that by going to lower methane/ethane ratio we improve material quality as seen in both XRD and PL. In terms of chemistry, this would mean that, of the two chemical reaction pathways to grow GaN-based material on the wafer, the surface reaction pathway with direct decomposition of the precursors (involving ethane byproduct) is preferred over the gas phase reaction pathway with complex adduct formation (involving methane byproduct). This was discussed in detail in our earlier work on real-time crystal quality prediction,<sup>20</sup> and it is reaffirmed here with the addition of PL results. Therefore, the results to date indicate that the surface reaction pathway, identified by its ethane byproduct, is the preferred route to grow high quality GaN-based material as verified by the two highly important post-process material characterization techniques—i.e., XRD and PL.

We also demonstrated here a contamination control methodology that assures a low gas phase impurity condition prior to material growth (Figs. 2–4). Implementing pre-growth reactor purge with high temperature and purging gas, and monitoring the reduction in the relevant gas phase impurity levels allowed us to guarantee acceptable product

quality as seen in postprocess PL. This is important because it provides an opportunity to implement the solution in a timely fashion (i.e., pregrowth as opposed to during growth) thus significantly increasing its effectiveness in terms of achieving acceptable material quality. In terms of the metrology precision presented here, it varied anywhere from  $\sim 5\%$  to  $\sim 19\%$  depending on the model. However, the goal here is not a precision course correction as done for other figures of merit such as the AlGaIn cap layer thickness control,<sup>19</sup> but a rather general fault detection that leads to routine contamination control to guarantee some required conditions before growth by preparing an acceptably low impurity growth environment. This is accompanied by detection of occasional process and equipment excursions as shown in Figs. 5–7.

## V. CONCLUSIONS

*In situ* mass spectrometry sensing was implemented in AlGaIn/GaN HEMT heterostructure growth processes to drive both FDC and course correction with the goal of enhancing and controlling process reproducibility. Dynamic chemical sensing through the entire process cycle, carried out downstream from the wafer, revealed generation of methane and ethane reaction byproducts in real time, in addition to other residual gas species present as impurities within the reactor. Using the methane/ethane ratio, material quality as measured by postprocess PL band-edge intensity was shown to be predictable in real time during growth with quantitative precision of  $\sim 5\%$ . This goes hand in hand with the previously demonstrated GaN epilayer crystal quality prediction (to  $\sim 5\%$  precision verified by postprocess XRD) using the same methane/ethane byproducts ratio.<sup>20</sup> Both correlations indicate that better quality material is obtained for lower methane/ethane ratio. They suggest that, of the two chemical reaction pathways to grow GaN, the surface reaction pathway with direct decomposition of the precursors (identified by the ethane byproduct) is preferred over the gas phase reaction pathway with adduct formation (identified by the methane byproduct).

Correlations seen between pregrowth gas phase impurity levels within the reactor and postprocess PL qualities suggested that low gas phase impurity condition is critical for high quality GaN material growth. Specifically, better quality material (as seen in higher band-edge intensity) was obtained when the pregrowth residual H<sub>2</sub>O level was lower, and better quality material (as seen in lower deep-level intensity) was obtained when the pregrowth residual O<sub>2</sub> level was lower. Based on these results a contamination control methodology was developed that assures a low gas phase impurity condition prior to material growth. Implementing pregrowth reactor purge with high temperature and purging gas, and monitoring the reduction in the relevant gas phase impurity levels allowed us to guarantee acceptable product quality as seen in postprocess PL. These real-time fault detection and contamination control activities have been accompanied by detection of the more infrequent process and equipment excursions.

In summary, real-time fault detection and contamination control based on impurity levels monitoring, combined with the course correction activities based on methane/ethane byproducts ratio<sup>20</sup> and the time-integrated film thickness metric,<sup>19</sup> have made significant contributions to our materials and process development efforts in terms of improved material quality and yield. These kinds of APC activities are now in routine use for the GaN-based semiconductor processes at Northrop Grumman Electronics Systems, with the prognosis for applications in other types of processes as well.

## ACKNOWLEDGMENTS

The authors are grateful for a close research partnership with, and financial support from, the Northrop Grumman Corporation. We also appreciate continuing interaction and technical support from Inficon, Inc., particularly R. Ellefson and L. Frees. Inficon is a supplier of mass spectrometric sensors for process control applications in semiconductor manufacturing processes.

<sup>1</sup>L. F. Eastman and U. K. Mishra, *IEEE Spectrum* **5**, 28 (2002).

<sup>2</sup>U. K. Mishra, P. Parikh, and Y. Wu, *Proc. IEEE* **90**, 1022 (2002).

<sup>3</sup>R. J. Trew, *Proc. IEEE* **90**, 1032 (2002).

<sup>4</sup>T. Sonderman, M. Miller, and C. Bode, *Future Fab International* **12**, 119 (2002).

<sup>5</sup>S. W. Butler, *J. Vac. Sci. Technol. B* **13**, 1917 (1995).

<sup>6</sup>L. L. Tedder, G. W. Rubloff, I. Shareef, M. Anderle, D.-H. Kim, and G. N. Parsons, *J. Vac. Sci. Technol. B* **13**, 1924 (1995).

<sup>7</sup>L. L. Tedder, G. W. Rubloff, B. F. Cohaghan, and G. N. Parsons, *J. Vac. Sci. Technol. A* **14**, 267 (1996).

<sup>8</sup>A. I. Chowdhury, W. W. Read, G. W. Rubloff, L. L. Tedder, and G. N. Parsons, *J. Vac. Sci. Technol. B* **15**, 127 (1997).

<sup>9</sup>G. Lu, L. L. Tedder, and G. W. Rubloff, *J. Vac. Sci. Technol. B* **17**, 1417 (1999).

<sup>10</sup>T. Gougousi, Y. Xu, J. N. Kidder, Jr., G. W. Rubloff, and C. R. Tilford, *J. Vac. Sci. Technol. B* **18**, 1352 (2000).

<sup>11</sup>L. Henn-Lecordier, J. N. Kidder, Jr., G. W. Rubloff, C. A. Gogol, and A. Wajid, *J. Vac. Sci. Technol. A* **19**, 621 (2001).

<sup>12</sup>R. Sreenivasan, T. Gougousi, Y. Xu, J. Kidder, Jr., E. Zafriou, and G. W. Rubloff, *J. Vac. Sci. Technol. B* **19**, 1931 (2001).

<sup>13</sup>Y. Xu, T. Gougousi, L. Henn-Lecordier, Y. Liu, S. Cho, and G. W. Rubloff, *J. Vac. Sci. Technol. B* **20**, 2351 (2002).

<sup>14</sup>L. Henn-Lecordier, J. N. Kidder, Jr., G. W. Rubloff, C. A. Gogol, and A. Wajid, *J. Vac. Sci. Technol. B* **21**, 1055 (2003).

<sup>15</sup>S. Cho, L. Henn-Lecordier, A. Singhal, Y. Xu, Y. Liu, J. N. Kidder, Jr., and G. W. Rubloff, *Proceedings AEC/APC Symposium XV*, edited by International Sematech (International Sematech, Austin, TX, 2003) (Cho\_Soon-SP2595).

<sup>16</sup>S. Cho, L. Henn-Lecordier, Y. Liu, and G. W. Rubloff, *J. Vac. Sci. Technol. B* **22**, 880 (2004).

<sup>17</sup>S. Cho, G. W. Rubloff, M. E. Aumer, D. B. Thomson, and D. P. Partlow, Presented at the AVS 50th International Symposium, Baltimore, MD, 2 November 2003 (unpublished).

<sup>18</sup>S. Cho, G. W. Rubloff, M. E. Aumer, D. B. Thomson, and D. P. Partlow, Presented at the MRS Fall Meeting, Boston, MA, 1 December 2003 (unpublished).

<sup>19</sup>S. Cho, D. S. Janiak, G. W. Rubloff, M. E. Aumer, D. B. Thomson, and D. P. Partlow, *J. Vac. Sci. Technol. B* (to be published).

<sup>20</sup>S. Cho, G. W. Rubloff, M. E. Aumer, D. B. Thomson, D. P. Partlow, and R. A. Adomaitis, *J. Vac. Sci. Technol. B* **23**, 1386 (2005).

<sup>21</sup>H. Morkoc, *Nitride Semiconductors and Devices* (Springer, Berlin, 1999), p. 159.

<sup>22</sup>L. Henn-Lecordier, J. N. Kidder, Jr., and G. W. Rubloff, *J. Vac. Sci. Technol. A* **22**, 1984 (2004).